International Journal of Microwave and Wireless Technologies, 2013, 5(3), 301–308.
doi:10.1017/S1759078713000536

RESEARCH PAPER

A proof of concept of a non-resonant near-field microwave microscope based on a high impedance reflectometer

DAVID GLAY, ADELHATIF EL FELLAHI AND TUAMI LASRI

In this paper, we present a non-resonant high impedance reflectometer with a reference impedance close to one of the tip probe of a near-field microwave microscope. We show that for an apex of the tip probe of 100 μm there is an optimum reference impedance close to 1 kΩ. To validate this approach a microwave circuit that makes use of lumped elements has been fabricated. A proof of concept is also explored for capacitance measurements between the tip probe and a metal plate.

Keywords: Characterization of material parameters, Circuit design and applications, Near-field microwave microscopy

Received 26 October 2012; Revised 23 April 2013; first published online 3 June 2013

I. INTRODUCTION

Most of the near-field microwave microscopy consists of employing a tip probe of sub-wavelength size and a sample that is placed in the near-field of the probe, so that the spatial resolution – both lateral and in-depth – is governed by the probe geometry size rather than by the wavelength [1, 2]. In the field of nanoscale technology typical impedance of the tip is usually in order of several kohms. Therefore, the overall challenge is to improve the accuracy in case of very high impedance measurements especially in high frequency range [3, 4].

Often, the purpose is to obtain material properties of the sample under test. Hence, there is a need for access to quantitative microwave measurements to extract the parameters of interest. In this context, several investigations have been conducted to propose solutions for microwave characterization at the nanometer scale.

Actually, to overcome these difficulties a number of techniques have been proposed in the literature over the past decade such as resonator matching networks [5–7], interferometric measurements [8, 9], high impedance Wheatstone bridges [10], or time domain measurements [11]. However, none of these methods allow both direct and non-resonant precise measurements. Incontestably, the resonant technique is considered as the most sensitive technique to relative variations of the load provided that a resonator with good quality factor is used. Nevertheless, this technique presents the major disadvantage not to be able to measure the absolute impedance of the load on a wide frequency band.

IEMN – University of Lille 1, Av. Poincaré – CS 60069, 59652 Villeneuve d'Ascq, France. Phone: + 33 (0)320197941
Corresponding author:
D. Glay
Email: david.glay@iemn.univ-lille1.fr

In this paper, we propose an alternative to the resonant method to overcome the frequency bandwidth limitation. The overall idea is to try to extend the microwave frequency bandwidth of operation while keeping enough sensitivity by using a non-resonant mode. The alternative proposed is based on the reduction of the mismatch that exists between the impedance of the probe and one of the measurement system. In fact, the new method developed in this study consists of bringing the reference impedance of measurement system close to the tip impedance. Hence, instead of looking at the changes in coupling coefficient in terms of shifts in frequency and quality factor we directly exploit the reflection coefficient.

Section II overviews the underlying principle of the system proposed. Section III discusses the realization of the system and experimental validation tests.

II. THEORY

Near-field microwave microscopy has become a popular technique to characterize the properties of nanoscale materials and devices at high frequency. It has been successfully used to quantitatively image metals, semiconductors, and dielectrics [12–14]. The basic principle consists of near-field interaction between a source and a sample. The antenna is a subwavelength probe. One of the strengths of near-field microscopy is that measurements can be performed without any physical contact between the tip and the sample to characterize.

It is well known that a tip probe in front of a sample can be modeled primarily as a resistance in series with a capacitance depending on the tested sample and the distance separating the sample and the tip apex. In many cases, especially at microwave frequencies, the effect of the resistance is low compared to the impedance of the capacitance close to a few tens of femtoFarad for a tip apex in the order of 100 μm. For apex sizes at the nanoscale, the capacitance may decrease to some attoFarad [9].

For example, a capacitance of 100 fF has a reactance of 1.6 kΩ at a frequency of 1 GHz. Hence, direct determination of the impedance by a traditional measure of its reflection coefficient is difficult because of the high contrast with conventional network analyzer impedance referenced to 50 Ω. To overcome this constraint, indirect methods using a resonator or interferometric techniques are used. These methods have the advantage of being very sensitive to sample variations. However, they are frequency selective and do not allow absolute characterization of the sample.

The original idea developed in this paper is to propose a non-resonant instrumentation with a reference impedance Z_o close to the one of the tip probe in order to directly characterize the sample under test through measurement of a reflection coefficient.

In the case of a tip probe modeled only by capacitance C, the reflection coefficient Γ_L is written as

$$\Gamma_L = \frac{1 - jZ_o C\omega}{1 + jZ_o C\omega}. \tag{1}$$

This expression shows that only the phase φ of Γ_L is usable since its magnitude is constant and equal to unity irrespective of the value of C. By a simple calculation using partial differential we obtain the capacitance measurement error δC depending on the phase error $\delta\varphi$ according to the expression

$$\delta C = -\frac{1 + (Z_o C\omega)^2}{2Z_o\omega}\delta\phi. \tag{2}$$

This equation, which is a parabolic function of Z_o, shows that for a pulsation ω and a capacitance C, the error in the measurement of capacitance depends obviously not only on the phase error but also on the reference impedance Z_o selected. We show, by calculating the derivative, that there is a particular value Z_o for which the measurement error δC is minimum. This optimal reference impedance is given by $Z_o = 1/C\omega$.

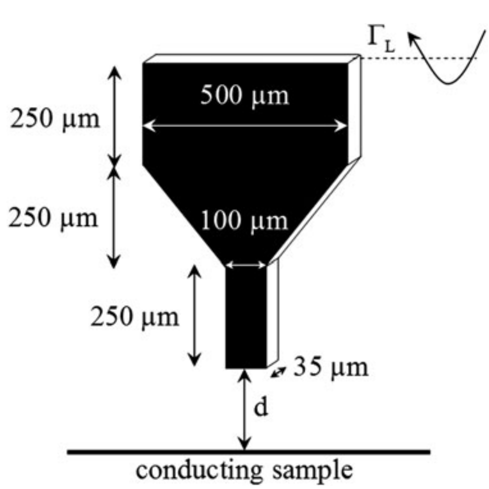

Fig. 1. Design of the probe on Epoxy FR4-1.6 mm substrate.

To show the influence of reference impedance Z_o on measurement uncertainty of a near-field microwave microscope, we propose an example of a tip probe designed by using micro-strip lines on Epoxy FR4-1.6 mm substrate (Fig. 1).

The probe is a very important part of the microscope. It is established that the resolution of the system is determined by the size of the probe and its distance from the sample. In this study, the resolution is not targeted, what is aimed at is the proof of concept of a new instrumentation that does not include resonators. Hence, in this work a simple design using a low cost technology is proposed.

By using a finite element method simulator, Ansoft HFSS, we can estimate the impedance of this probe located at a distance d of a conducting plate. In Fig. 2, the capacitance observed between the probe and the conducting plate for distances going from 1 μm to 5 mm is represented.

The figure shows logarithmic increase of capacitance versus decrease of tip probe-conducting sample distance in the range of 5–500 μm (slope = −18.3 fF/decade). In the particular case of this probe (Fig. 1), we observe that the retrieved capacitance changes between about 40 and 100 fF. Finally, one can see that for a stand-off distance greater than 1 mm, the capacitance remains constant and corresponds to the micro-strip open-ended capacitance estimated to be 40 fF from high frequency structure simulator (HFSS) simulations.

From these simulation results, we present in Fig. 3 the uncertainty on the capacitance versus the reference impedance Z_o for a reflection coefficient phase error of 0.1 degree by using equation (2). In this study, we first consider a constant frequency ($F = 2$ GHz) and the capacitance is varied from 40 to 100 fF (Fig. 3(a)). Then, we estimate the error on the capacitance ($C = 100$ fF) when the frequency varied from 500 MHz to 2 GHz (Fig. 3(b)).

These results show that for a reference impedance Z_o around 1 kΩ, variations as well of the capacitance as of the frequency used do not greatly affect measurement accuracy. Thus, we propose to design a non-resonant measurement system with reference impedance Z_o fixed at 1 kΩ for measurement of reflection coefficients.

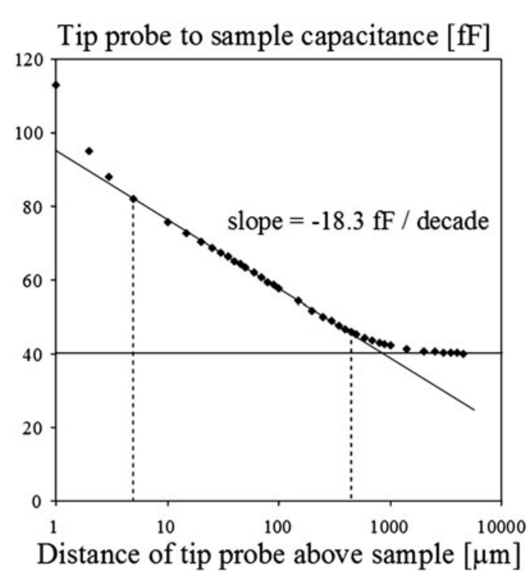

Fig. 2. Tip-sample capacitance versus tip-conducting sample distance (HFSS simulations).

https://doi.org/10.1017/S1759078713000536 Published online by Cambridge University Press

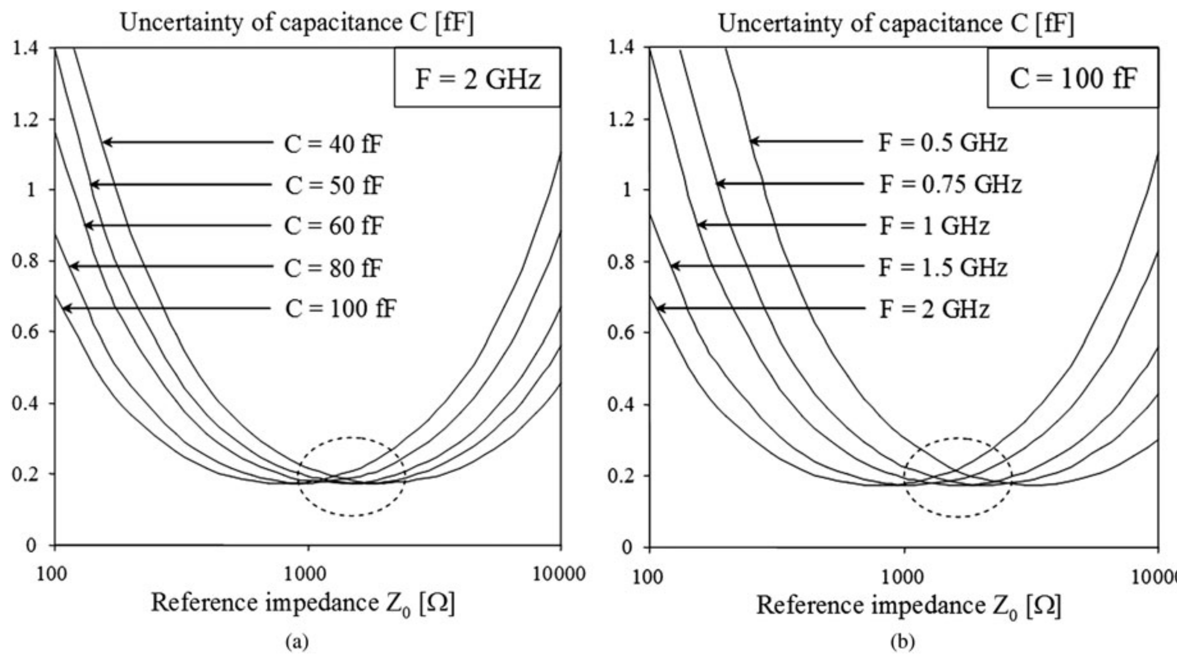

Fig. 3. Uncertainty of capacitance C versus reference impedance Z_0.

To do this we strive to reduce the use of reactive elements, such as for example the propagation lines, for benefit of resistive elements [15]. Thus, to form a high impedance reflectometer (HIR), we propose to combine a conventional two-port Vector Network Analyzer (VNA) to a high reference impedance splitter via two impedance matching networks (Fig. 4).

In Fig. 5, we show the schematic and the flow graph of the HIR conceived by considering that the matching networks are made of two resistors ($R_1 = 50\ \Omega$ and $R_2 = 1\ \mathrm{k}\Omega$). The power divider is based on an Owen splitter [16]. The two resistors are defined to realize a good compromise between coupling factor and isolation ($R_3 = 1.33\ \mathrm{k}\Omega$ and $R_4 = 2\ \mathrm{k}\Omega$).

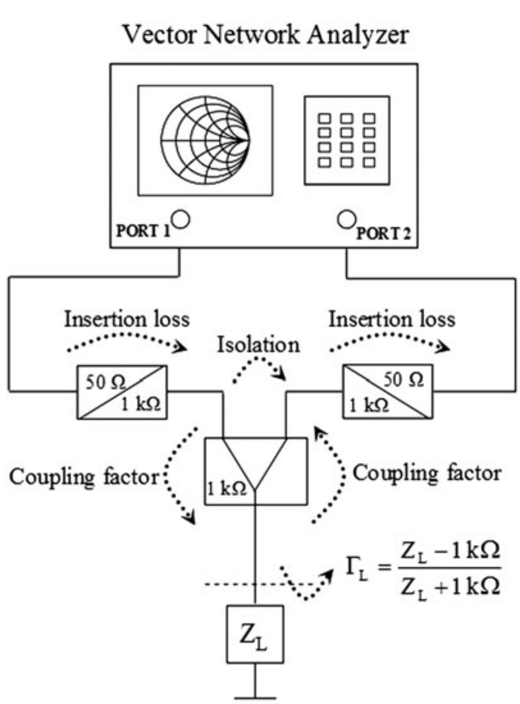

Fig. 4. Bloc diagram of HIR connected to Z_L.

By taking into account only all first-order loops, the transmission coefficient S_{21} derived from the signal flow graph technique can be written as:

$$S_{21} = \frac{T_1^2[T_2(1-\Gamma_L\Gamma_4)+T_3^2\Gamma_L]}{1-2\Gamma_2\Gamma_3-T_2^2\Gamma_2^2-\Gamma_4\Gamma_L-2T_3^2\Gamma_2\Gamma_L}, \qquad (3)$$

where the complex reflection coefficient Γ_L is defined by (1).

It has to be noted that the reference impedance is 50 Ω for Γ_1, whereas it is 1 kΩ for Γ_2, Γ_3, Γ_4, and Γ_L. Hence, in ideal case $\Gamma_1 = 0$, $\Gamma_2 = \Gamma_3 = \Gamma_4 = 0$, and $T_2 = T_3^2$. From these considerations, the transmission coefficient S_{21} can be written as:

$$S_{21} = \frac{2T_1^2 T_2}{1 + jZ_0C\omega}, \qquad (4)$$

where T_1, T_2, and T_3 represent respectively the matching network insertion loss, isolation, and coupling factor of the splitter. The different simulations performed lead to the following findings: $|T_1| = -19.1$ dB, $|T_2| = -19$ dB, and $|T_3| = -9.5$ dB.

Given the low capacitance values considered, equation (4) shows that the magnitude of S_{21} is almost insensitive to the variation of capacitance C and remains close to -51 dB.

Assuming that the matching networks and the power splitter are made with perfect resistors, T_1, T_2, and T_3 can be considered purely real. Hence, we can approximate the phase of the transmission coefficient by

$$\arg(S_{21}) = -\mathrm{atan}(Z_0C\omega). \qquad (5)$$

From HFSS simulations of the reflection coefficient Γ_L referenced to 1 kΩ, we can give the evolution of S_{21} phase-

https://doi.org/10.1017/S1759078713000536 Published online by Cambridge University Press

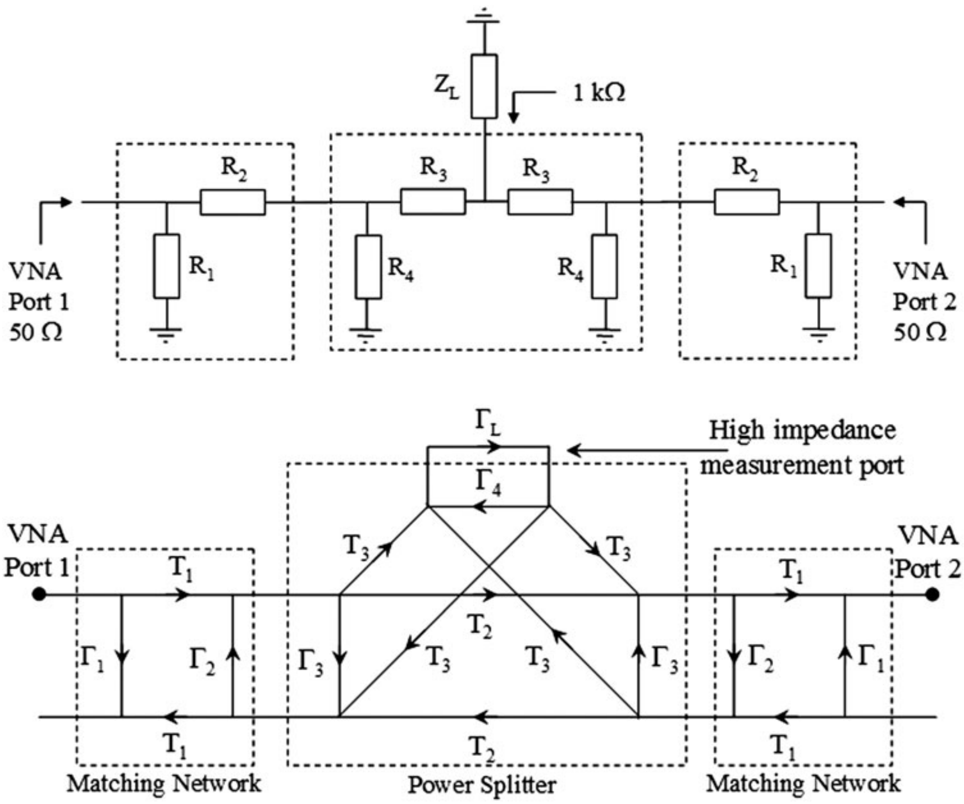

Fig. 5. Schematic and signal flow graph of HIR connected to Z_L.

shift versus frequency for several tip-conducting sample distances (Fig. 6). We also report the corresponding value of the capacitance from equation (5).

This simulation shows a change in the S_{21} phase-shift which is large enough to distinguish a variation of capacitance in the range of 40–100 fF. However, to increase the measurement accuracy, instead of determining the capacitance for a particular frequency, the idea is to take advantage of the non-resonant nature of the measurement system by fitting equation (5) in the frequency band considered.

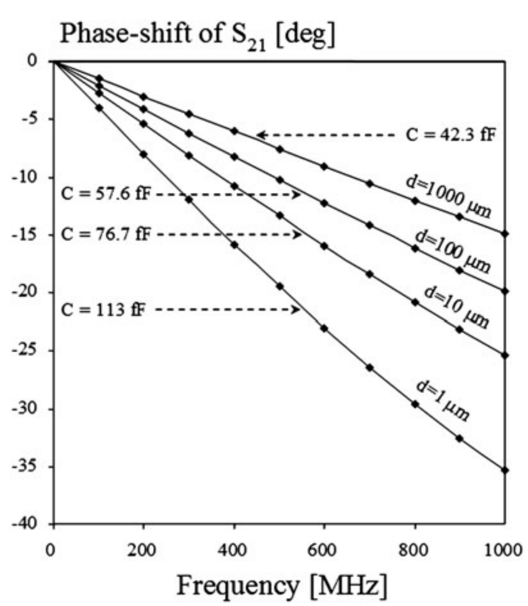

Fig. 6. S_{21} phase-shift versus frequency for different tip-conducting sample distances.

In the next section we present a microwave measurement system with high reference impedance Z_0 equal to 1 kΩ.

III. FABRICATION AND EXPERIMENTAL RESULTS

The main problem to develop broadband systems with high characteristic impedance is the difficulty to realize micro-strip lines with high impedance. Thus, to achieve the high reference impedance splitter and the impedance matching networks, we propose to use only resistive lumped elements. Nevertheless, particular attention should be given to reduce connections between these components [17].

As has already been mentioned the objective of this study is not system performance. Features like resolution or high frequency functioning are not the priority of our investigation. The aim is to demonstrate the possibility to achieve near-field microwave microscopy by means of an original high impedance system. Thus, each function of our system is realized using resistive elements in boxes SMD 0402 mounted on Epoxy FR4-1.6 mm substrate.

Owing to the unavoidable propagation phenomena and parasitic capacitance cut-off effect limits of resistors, we restrict the validation tests to a frequency of 500 MHz. To demonstrate these limitation effects, we present in Fig. 7, equivalent impedance (real and imaginary parts) versus frequency of several SMD 0402 resistance values $R = 50\ \Omega$ (Fig. 7(a)), $R = 1\ k\Omega$ (Fig. 7(b)) and $R = 2\ k\Omega$ (Fig. 7(c)). Typical value of the internal shunt capacitance is around 40 fF.

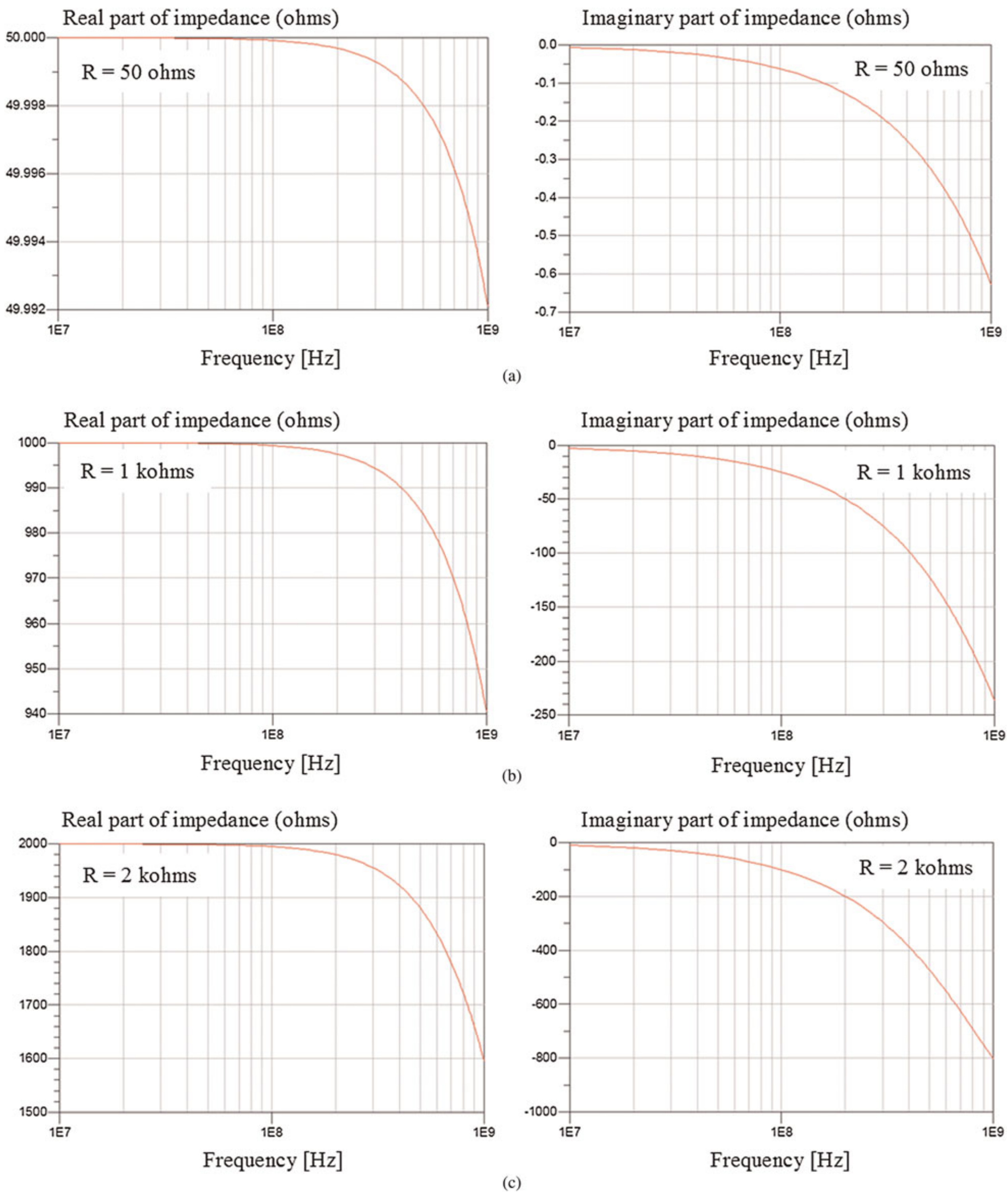

Fig. 7. Equivalent impedance versus frequency of several SMD 0402 resistance values.

The results exhibit that for 50 Ω SMD 0402 resistance, operation up to 1 GHz poses no problem. However, for resistance values of 1 kΩ and 2 kΩ, the results show that in particular the imaginary part is not negligible even for frequencies as low as 100 MHz. We are aware, from these curves that the resistances that are used for the splitter and matching networks are far from perfect especially in microwave. Nevertheless, to prove the concept up to a few hundred MHz, this low-cost technology is sufficient.

In order to measure the characteristics of the resistive matching network, we combine two networks in series so as to be compatible with the impedance 50 Ω of VNA ports. Figure 8 presents the photography of the circuit and the experimental results showing a non-resonant matching impedance ($|S_{11}| < -20$ dB) and a relatively constant evolution of $|S_{21}|$ up to a frequency of 500 MHz.

As the two networks are in series one can estimate the insertion loss of only one matching network to

https://doi.org/10.1017/S1759078713000536 Published online by Cambridge University Press

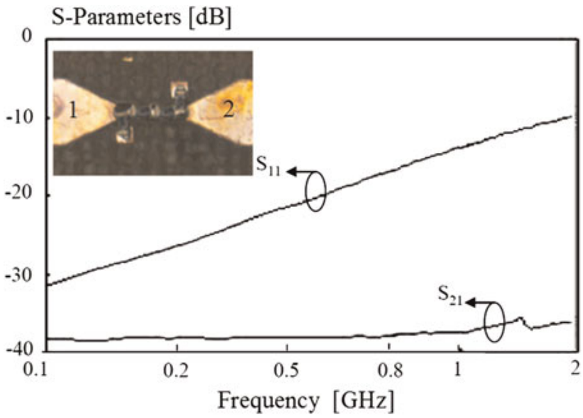

Fig. 8. Resistive matching networks: photography and experimental results.

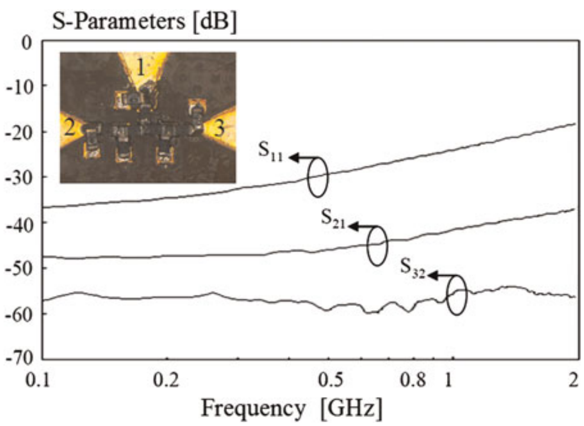

Fig. 9. Power splitter with resistive matching networks: photography and experimental results.

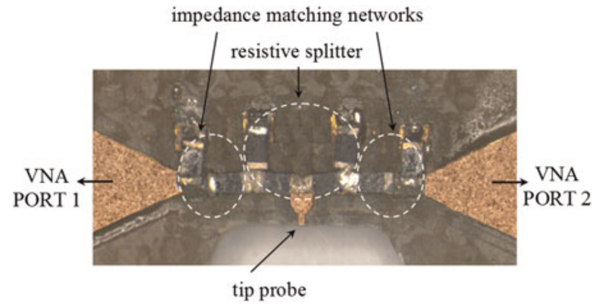

Fig. 10. HMIC part of the near-field microwave microscope.

−19.1 dB, corresponding to the theoretical value given in Section II.

In the same way, concerning the characterization of the high impedance splitter, we have placed in front of each access a resistive matching network in order to be compatible with the VNA in terms of impedance. We present in Fig. 9 the photography of the circuit and the experimental results showing a non-resonant matching impedance ($|S_{11}| < -30$ dB) and relatively constant evolutions of $|S_{21}|$ and $|S_{32}|$ up to a frequency of 500 MHz.

It has to be mentioned that the resistance values that have been selected to build the splitter are somewhat different to those calculated. These resistances are $R_3 = 1.2$ kΩ and $R_4 = 1.8$ kΩ instead of $R_3 = 1.33$ kΩ and $R_4 = 2$ kΩ.

By considering that insertion loss of the resistive matching networks is equal to −19.1 dB, one can estimate the high impedance splitter parameters. We found out a coupling factor equal to −9.8 dB from S_{21} and an isolation equal to −17.8 dB from S_{32}.

Thus, by combining a VNA with two matching networks and a power splitter, as presented in Fig. 4, we obtain an HIR allowing us to measure a reflection coefficient Γ_L with a referenced impedance of 1 kΩ.

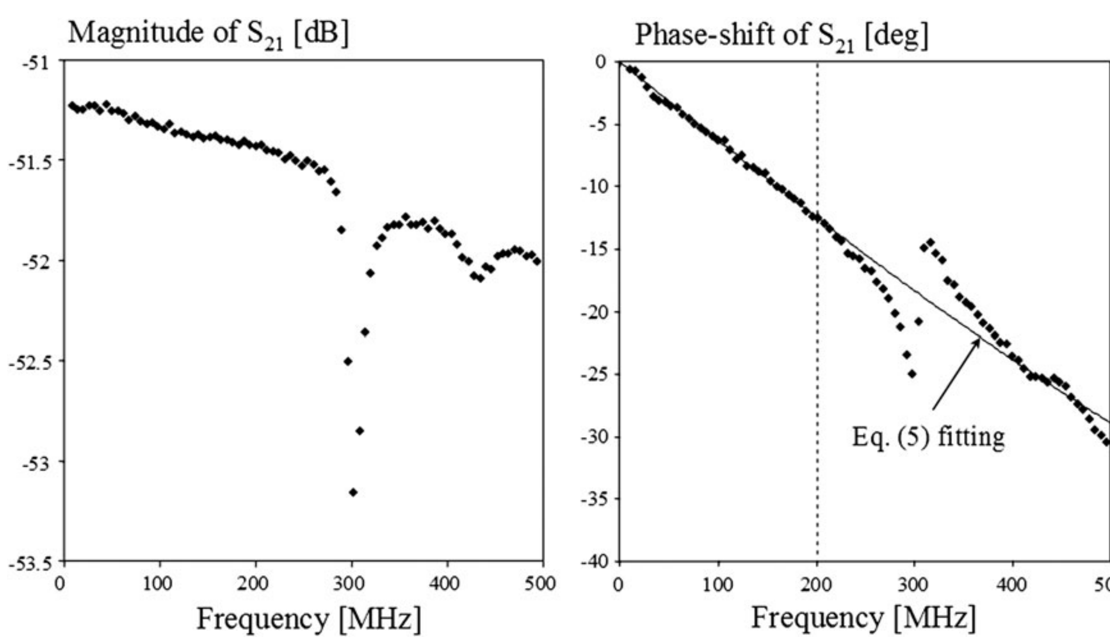

Fig. 11. S_{21} magnitude and phase-shift evolutions versus frequency.

https://doi.org/10.1017/S1759078713000536 Published online by Cambridge University Press

To realize the microscope, a probe is associated with this set-up. The microwave circuit part of the near-field microscope is fabricated using hybrid microwave integrated circuit (HMIC) process, where the tip probe (apex = 100 μm) is directly mounted on the circuit (Fig. 10).

Transitions from SubMiniature version A (SMA)-Connector to micro-strip line on Epoxy FR4 1.6 mm substrate are used to connect the VNA R&S® ZVL6 via coaxial cables.

The first experiment that is conducted consists of measuring the transmission coefficient when the probe is in air (without sample under test). In Fig. 11, experimental data of the magnitude and the phase-shift of S_{21} versus the frequency allow us to emphasize a capacitive behavior.

The results show that the magnitude of the transmission coefficient is quite constant up to 200 MHz (around −51.2 dB). Concerning the phase-shift, a response relatively linear with the frequency (such as equation (5), where $Z_0C\omega \ll 1$) is observed up to 200 MHz. Above this frequency, there is a resonance phenomenon certainly due to the parasitic elements brought by resistors SMD 0402 boxes.

An estimation of the tip probe to sample capacitance can be easily obtained by inversion of the model given by equation (5).

$$C = \frac{-\tan\left[\arg(S_{21})\right]}{Z_0\omega}. \tag{6}$$

However, weak variations of the capacitance C induced by weak variations of distance d do not offer a sufficiently large phase-shift to guarantee good measurement accuracy by using directly the predictive model (equation 6). Indeed, representation of the S_{21} phase-shift versus frequency for different distance d, evolving between 50 and 300 μm exhibit small variations (Fig. 12).

To increase the phase-shift measurement accuracy, we will take advantage of the non-resonant nature of the system.

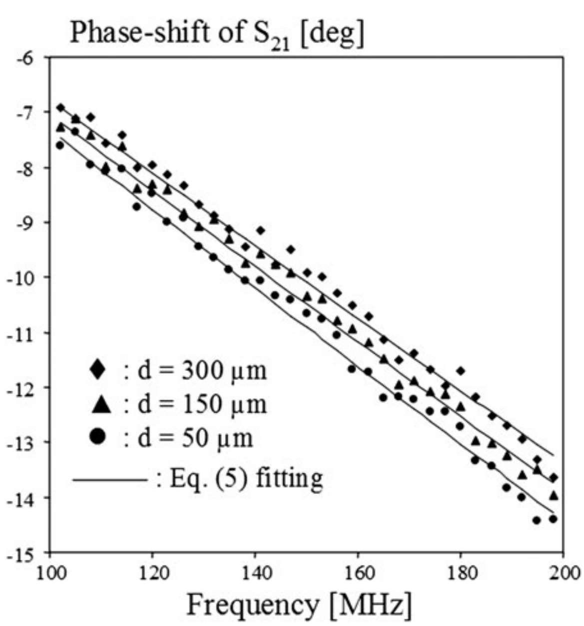

Fig. 12. Measurement of S_{21} phase-shift evolution versus frequency for different distance d.

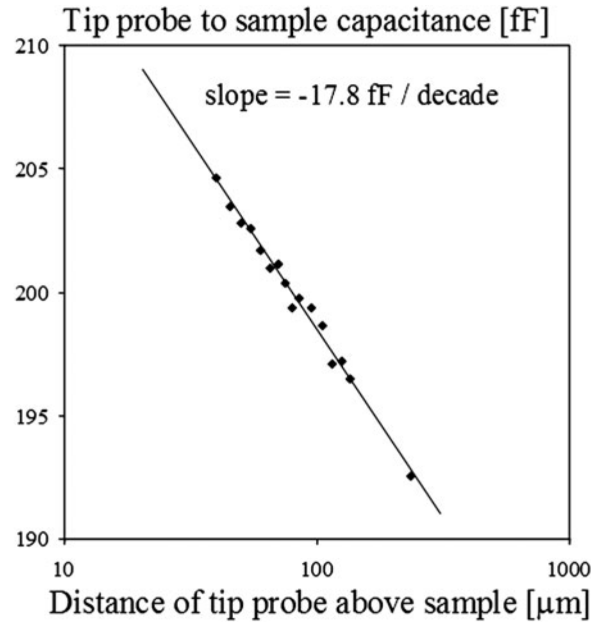

Fig. 13. Measurement of the tip probe to sample capacitance versus tip-sample distance.

Hence, the transmission coefficient is not measured for only one frequency but in a frequency band. Therefore, to estimate the capacitance C, we have made a linear fitting of the function $\tan[\arg(S_{21})]$ on the frequency range [10–200 MHz] (Fig. 12). These results show that we still can differentiate and quantify variations in capacitance between 50 and 300 μm without any ambiguity.

As has already been shown in Fig. 2, one can note in Fig. 13 the logarithmic increase of capacitance versus decreasing tip-sample distance. We notice a very good agreement between the slopes observed for measurements (slope = −17.8 fF/decade) and HFSS simulations (slope = −18.3 fF/decade). The offset is mainly due to the equivalent capacity of the HIR which is not taken into account in HFSS simulations.

Through this example, we demonstrate that our non-resonant method, using a multi-frequency approach (up to 200 MHz in this case), is sensitive enough to distinguish capacitances around 200 fF with an error estimated to 0.5 fF.

IV. CONCLUSION

We present a non-resonant high reference impedance reflectometer matched to a tip probe dedicated to near-field microwave microscopy. We show that for a tip probe of a particular size (micrometric size in this study) it is possible to define an optimum reference impedance reflectometer integrating the tip probe. The realization in HMIC process by using SMD 0402 resistors is used as proof of concept. To increase frequency band, monolithic microwave integrated circuits (MMIC) technology is certainly a better solution to reduce parasitic effects of resistors and propagation phenomena. Many potential applications can be addressed, in particular quantitative probing of local complex permittivity of materials is of interest. For example, wafers inspection in microelectronics industry could be an interesting field to investigate by using this technology.

REFERENCES

[1] Gao, C.; Xiang, X.-D.: Quantitative microwave near-field microscopy of dielectric properties. Rev. Sci. Instrum., **69** (11) (1998), 3846–3851.

[2] Anlage, S.M.; Talanov, V.V.; Schwartz, A.R.: Principles of Near-Field Microwave Microscopy, Scanning Probe Microscopy: Electrical and Electromechanical Phenomena at the Nanoscale, vol. **I**, S.K. Kalinin and A. Gruverman (Ed.), Springer–Verlag, New York, ISBN: 978-0-387-28667-9, 2007, 215–253.

[3] Rouhi, N.; Jain, D.; Burke, P.J.: Nanoscale devices for large-scale applications. IEEE Microw. Mag., **11** (7) (2010), 72–80.

[4] Imtiaz, A.; Pollak, M.; Anlage, S.M.: Near-field microwave microscopy on nanometer length scales. J. Appl. Phys., **97** (4) (2005), 044302.1–044302.6.

[5] Weber, J.C. et al.: A near-field scanning microwave microscope for characterization of inhomogeneous photovoltaics. Rev. Sci. Instrum., **83** (2012), 083702.1–083702.7.

[6] Kharkovsky, S. et al.: Microwave resonant switched-slot probe with perpendicular coaxial feed, in Proc. of IEEE Instrumentation and Measurement Technology Conf. (I2MTC), May 2010, 1299–1303.

[7] Chisum, J.D.; Popović, Z.: Performance limitations and measurement analysis of a near-field microwave microscope for nondestructive and subsurface detection. IEEE Trans. Microw. Theory Tech., **60** (8) (2012), 2605–2615.

[8] Randus, M.; Hoffmann, K.: A method for direct impedance measurement in microwave and millimeter-wave bands. IEEE Trans. Microw. Theory Tech., **59** (8) (2011), 2123–2130.

[9] Huber, H.P. et al.: Calibrated nanoscale dopant profiling using a scanning microwave microscope. J. Appl. Phys., **111** (2012), 014301.1–014301.9.

[10] Nougaret, L. et al.: Gigahertz characterization of a single carbon nanotube. Appl.Phys. Lett., **96** (4) (2010), 042109.1–042109.3.

[11] Chen, F.; Chandrakasan, A.; Stojanovic, V.: An oscilloscope array for high-impedance device characterization. IEEE Proc. ESSCIRC, **11** (7) (2009), 112–115.

[12] Usanov, D.A. et al.: Microwave imaging of the ceramic plate surface with the nanometer metal layer by means of the near-field microscope based on the gunn-diode oscillator, in Proc. 41st European Microwave Conf. (EuMC), October 2011, pp. 210–213.

[13] Imtiaz, A.; Baldwin, T.; Nembach, H.T.; Wallis, T.M.; Kabos, P.: Near-field microwave microscope measurements to characterize bulk material properties. Appl. Phys. Lett., **90** (2007), 243105.1–243105.3.

[14] Imtiaz, A. et al.: Frequency-Selective Contrast on Variably Doped P-Type Silicon with a Scanning Microwave Microscope. J. Appl. Phys., **111** (2012) 093727.1–093727.6.

[15] El Fellahi, A.; Glay, D.; Haddadi, K.; Lasri, T.: High impedance RF four-port reflectometer, in Proc. 41st European Microwave Conf. (EuMC), October 2011, 491–494.

[16] Owen, C.: Owen Resistive Splitter, May 2007. [Online] http://www.microwaves101.com/encyclopedia/Resistive_splitter2.cfm

[17] Glay, D.; El Fellahi, A.; Lasri, T.: High impedance reflectometer dedicated to non-resonant near-field microwave microscopy, in Proc. 42nd European Microwave Conf. (EuMC), November 2012.

David Glay received the Engineer degree and the Ph.D. degree from the University of Lille 1, France, in 1995 and 1999, respectively. He is an Associate Professor of Electronics and Electrical Engineering in the University of Lille 1. His research topics are developed within the Institut d'Electronique, de Microélectronique et de Nanotechnologie (IEMN). New technological approaches based on microwaves and millimeter waves techniques, for non-destructive evaluation of materials and more generally of complex structures are studied. These last years, his research is more particularly related to the definition and the development of new broadband six-port based homodyne systems dedicated to nano-characterization in microwave and millimeter wave bands.

Adelhatif El Fellahi received the Master Degree in Advanced Technologies for Telecommunications and Mobility in 2008 at the University of Lille 1, where he is currently working toward the PhD Degree. His area of research concerns the definition and realization of a system for microwave characterization.

Tuami Lasri received the Ph.D. degree in electronics from the University of Lille 1, Villeneuve d'Ascq, France, in 1992. He is currently a Professor of Electronics and Electrical Engineering in the University of Lille 1. His main research interests, in the Institut d'Electronique, de Microélectronique et de Nanotechnologie (IEMN), encompass the development of measurement techniques, and the conception and realization of systems for microwave and millimeter wave non-destructive evaluation (NDE) purposes, including the characterization of nano-devices. Another interest in the area of electromagnetic wave interactions with materials concerns modeling of electromagnetic signals in high-loss and low-loss materials, homogeneous, multilayered, and heterogeneous dielectric systems. Recently, he has been involved in studies in the area of energy with the development of microgenerators based on thermoelectric transduction.

https://doi.org/10.1017/S1759078713000536 Published online by Cambridge University Press